

Alarmin S100A11 initiates a chemokine response to the human pathogen *Toxoplasma gondii*

Alexandra Safronova¹, Alessandra Araujo¹, Ellie T. Camanzo¹, Taylor J. Moon¹, Michael R. Elliott¹, Daniel P. Beiting² and Felix Yarovinsky^{1*}

***Toxoplasma gondii* is a common protozoan parasite that infects up to one third of the world's population. Notably, very little is known about innate immune sensing mechanisms for this obligate intracellular parasite by human cells. Here, by applying an unbiased biochemical screening approach, we show that human monocytes recognized the presence of *T. gondii* infection by detecting the alarmin S100A11 protein, which is released from parasite-infected cells via caspase-1-dependent mechanisms. S100A11 induced a potent chemokine response to *T. gondii* by engaging its receptor RAGE, and regulated monocyte recruitment in vivo by inducing expression of the chemokine CCL2. Our experiments reveal a sensing system for *T. gondii* by human cells that is based on the detection of infection-mediated release of S100A11 and RAGE-dependent induction of CCL2, a crucial chemokine required for host resistance to the parasite.**

Innate sensing of infection is important for triggering host defenses against invading pathogens, including protozoan parasites^{1,2}. Among various classes of innate immune sensors, Toll-like receptors (TLRs) have a central role in initiating interleukin 12 (IL-12)-dependent immune responses to pathogens¹. Both humans and mice share similar TLRs required for the recognition of conserved and essential bacterial and viral molecules, including the structural components of bacterial cell walls, RNA and DNA^{1,3}. However, the initial steps involved in recognition of the common protozoan parasite *Toxoplasma gondii* are vastly different in mice than in humans^{4,5}. In mice, recognition of the parasite is mediated by TLR11, which directly interacts with *T. gondii* profilin, a key molecule required for invasion of host cells by the parasite^{6,7}. *T. gondii* profilin is a classical pathogen-associated molecular pattern protein that is unique for *T. gondii* and other phylogenetically related apicomplexan parasites, including malaria and cryptosporidium⁶. Profilin is essential for *T. gondii* survival due to its nonredundant and essential role in regulating actin polymerization during obligate intracellular parasite entry into host cells⁷. Direct interactions between *T. gondii* profilin and the TLR11–TLR12 heterodimer complex lead to the induction of IL-12 and CCL2 via the adaptor MyD88 (myeloid differentiation primary response 88)–dependent signaling pathway^{8–11}. Both IL-12 and CCL2 are essential for host resistance to *T. gondii* in mice, and the lack of this cytokine and chemokine, respectively, leads to acute susceptibility to the infection^{4,12}. In marked contrast to the murine system, the initial steps for *T. gondii* recognition by human cells remain largely unknown due to a lack of functional genes encoding the key innate sensors TLR11 and TLR12 in the human genome¹³. *TLR11* is a pseudogene, and the gene encoding TLR12, which can form a heterodimer with TLR11 (refs^{8–10}), is not present in the human genome¹⁴. It is also unknown whether *T. gondii* profilin can be recognized by human cells. Although additional innate immune sensors, including TLR2, TLR4, NLRP1 (NOD-, LRR- and pyrin domain-containing 1) and NLRP3, can be activated by the parasite, they all have largely dispensable roles in the regulation of host defense and cytokine production^{4,15–17}. Thus, although up to one third of the world's population

is infected with *T. gondii* and has established a long-lasting immunity to the parasite¹⁸, how human innate immune cells recognize the parasite remains largely unknown.

RESULTS

***Toxoplasma gondii* triggers human CCL2 response.** Myeloid cells are sentinels of the immune system and are present in the blood and lymphoid organs and across many tissues. These cells are involved in early interactions with *T. gondii*¹⁹, and we hypothesized that they can recognize the parasite and induce protective innate immune responses. Lack of knowledge about the human cell types involved in *T. gondii* recognition prompted us to apply a systems biology approach with peripheral human blood cells comprising multiple hematopoietic cells. We aimed to decipher the human innate immune defense program by identifying the mediator of host defense triggered by the parasite.

An unbiased RNA-sequencing (RNA-seq) analysis of human peripheral blood cells revealed that innate responses to *T. gondii* were primarily characterized by the induction of chemokine expression, including that of *CCL2*, rather than by the induction of IL-12; this was evident from the low induction of *IL12B* and *IL12A* (Fig. 1a,b and Supplementary Fig. 1). These results were observed irrespective of which common laboratory *T. gondii* strain was used for experimental infection (RH88 or Pru).

Quantitative real-time PCR (rtPCR) analysis of *CCL2* and *IL12B* expression confirmed the screening results and established that *T. gondii* infection of human blood cells leads to much greater induction of *CCL2* than of *IL12B* (Fig. 1c).

Although our results indicate that induction of *CCL2* expression is a common effector mechanism downstream of innate parasite recognition by human cells, we also observed that there were differences in Pru and RH88 strain-mediated induction of chemokine responses (Fig. 1 and Supplementary Fig. 1). This observation is most likely due to the differences in virulence factors capable of regulating chemokine response in the infected cells and the pathogenicity of the *T. gondii* strains^{20–23}.

¹Center for Vaccine Biology and Immunology, Department of Microbiology and Immunology, University of Rochester Medical Center, Rochester, NY, USA.

²Department of Pathobiology, School of Veterinary Medicine, University of Pennsylvania, Philadelphia, PA, USA. *e-mail: felix_yarovinsky@urmc.rochester.edu

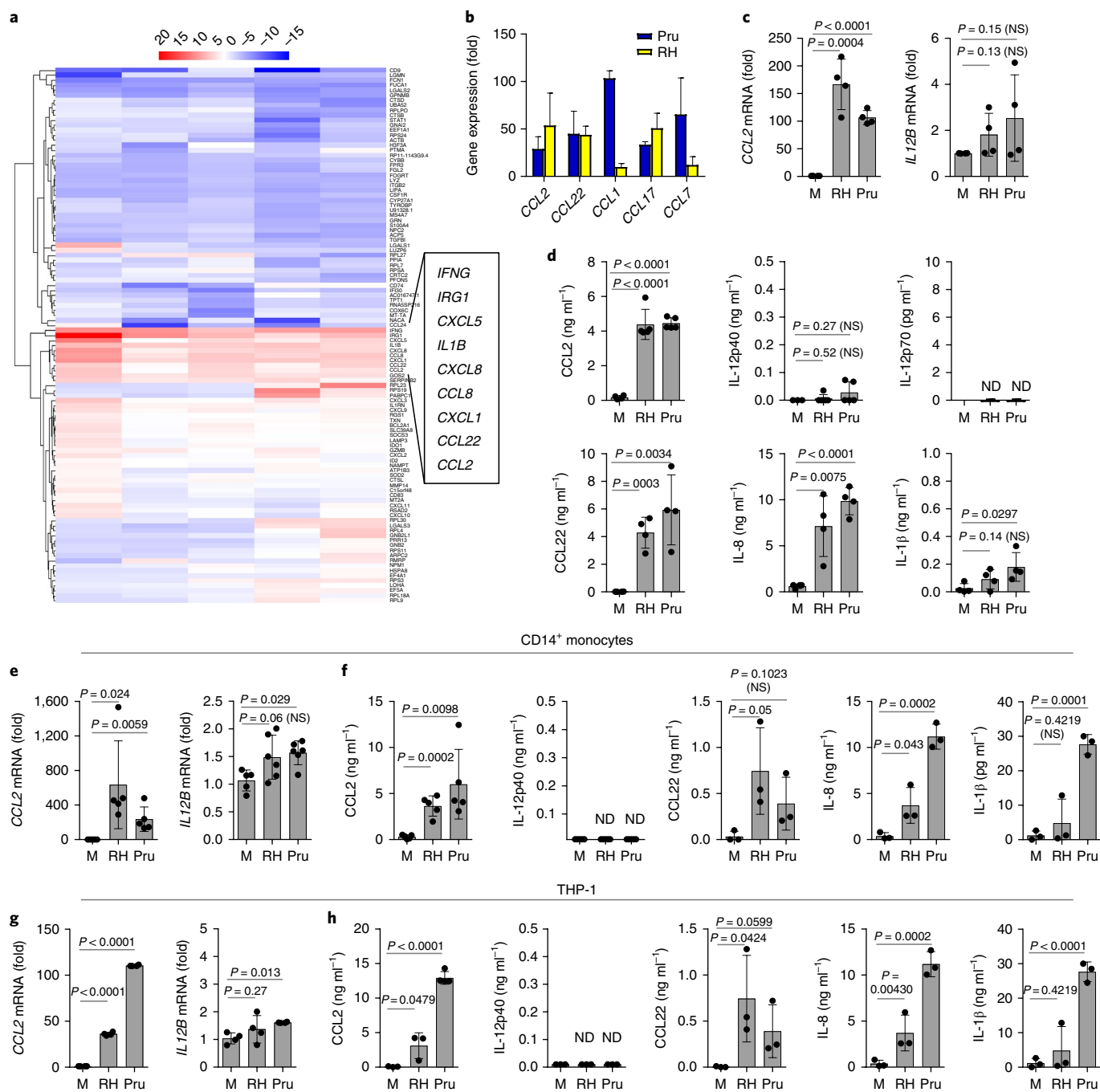


Fig. 1 | Transcriptome analysis identifies CCL2 as a signature response to *T. gondii* infection. **a**, Global gene transcriptome analysis of human PBMCs ($n=5$) infected with Pru tachyzoites (MOI, 3:1) for 12 h. RNA samples were collected and analyzed by RNA-seq. **b**, Analysis of chemokine expression in PBMCs ($n=5$) exposed to Pru (blue bars) and RH88 (RH, yellow bars) strains of *T. gondii* by RNA-seq. **c**, Quantitative rtPCR analysis for *CCL2* and *IL12B* expression in human PBMCs ($n=4$) infected with Pru and RH88 strains of *T. gondii*. **d**, Production of CCL2, IL-12p40, IL-12p70, CCL22, IL-8 and IL-1β by human PBMCs ($n=4$) infected with Pru and RH88 strains of *T. gondii*. M, media only (control). **e, f**, Analysis of *CCL2* and *IL12B* expression (**e**) and CCL2, IL-12p40, IL-12p70, CCL22, IL-8 and IL-1β secretion (**f**) in purified human CD14⁺ monocytes infected with Pru or RH88 strains of *T. gondii*. **g**, Expression of *CCL2* and *IL12B* in *T. gondii*-infected THP-1 cells. **h**, Secretion of CCL2, IL-12p40, IL-12p70, CCL22, IL-8 and IL-1β by THP-1 cells infected with Pru and RH88 strains of *T. gondii*. The data shown are representative of three (**a, b**), five (**c, d, g, h**) and four (**e, f**) independent experiments; error bars represent mean \pm s.d. Each symbol represents an individual PBMC sample (**c, d**), CD14⁺ monocytes isolated from an individual donor (**e, f**) or an individual cell culture well with THP-1 cells (**g, h**). Unpaired two-tailed Student's *t*-test was used for statistical analysis; NS, not significant; ND, not detected.

Human peripheral blood mononuclear cells (PBMCs) secreted large amounts of CCL2, CCL22 and IL-8 protein, but not IL-12 or IL-1β (Fig. 1d). Furthermore, we observed that the human monocyte cell line THP-1 induced high expression of *CCL2* (Fig. 1g) and

production of CCL2 protein in response to *T. gondii*, similarly to PBMCs and primary monocytes (Fig. 1e–h). This observation suggests that the human recognition system for the parasite is distinct from the mouse recognition system, which leads to IL-12 production

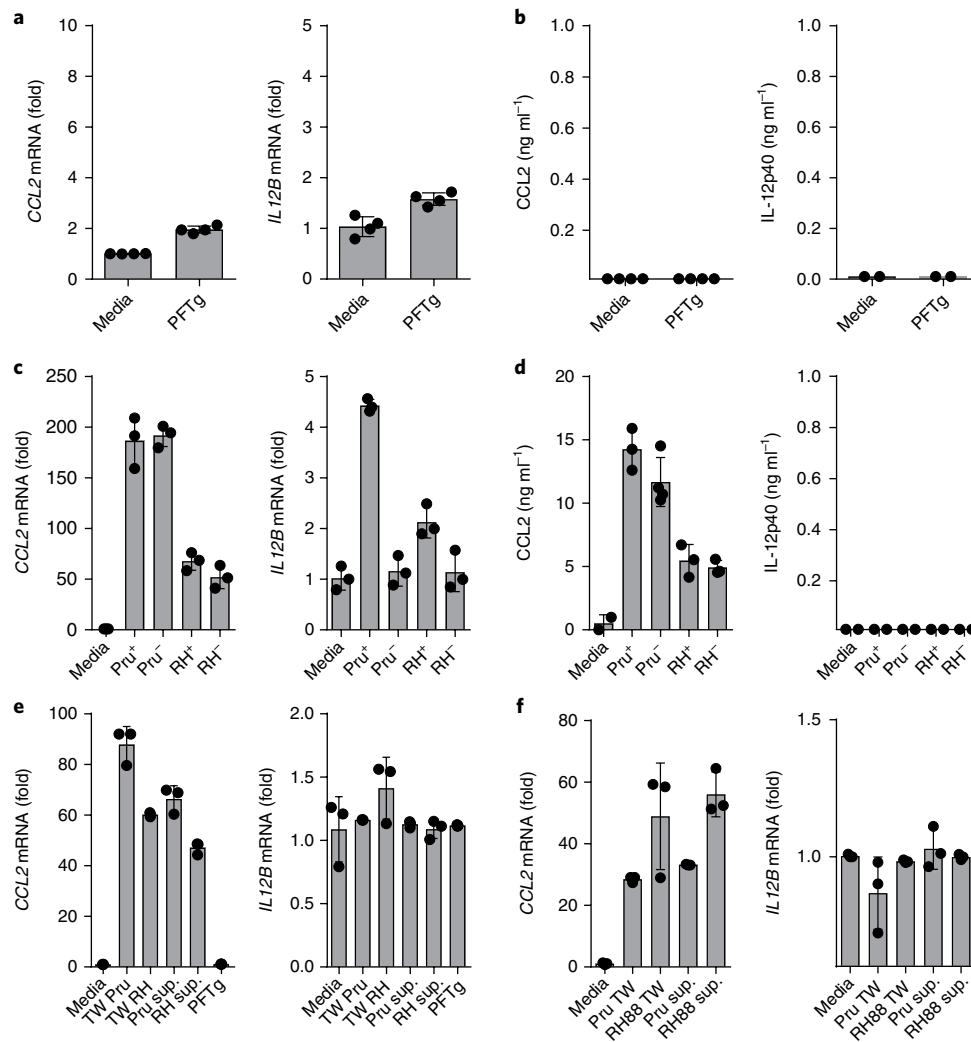


Fig. 2 | Soluble mediator elicits CCL2 production in response to *T. gondii* infection. **a,b**, Lack of *CCL2* and *IL12B* induction (**a**) and secretion (**b**) in THP-1 cells stimulated with purified *T. gondii* profilin (PFTg). **c**, THP-1 cells infected with mCherry-expressing Pru and RH88 strains of *T. gondii* were purified as infected cells (Pru⁺ and RH⁺) and uninfected cells (Pru⁻ and RH⁻). Expression of *CCL2* and *IL12B* was measured by rtPCR. **d**, Protein secretion of CCL2 and IL-12p40 was measured by ELISA. **e**, Analysis of *CCL2* and *IL12B* expression in THP-1 cells exposed to soluble mediators in a transwell system (TW) or by direct stimulation with cell culture supernatants collected from infected monocytes. **f**, Analysis of *CCL2* and *IL12B* expression in THP-1 cells exposed to soluble mediators in a transwell system (TW) with infected fibroblasts or by direct stimulation with cell culture supernatants (sup.) collected from infected fibroblasts. Each symbol represents an individual experimental sample. $n=4$ (**a,b**); $n=3$ (**c-f**). Data represent five independent experiments; error bars represent mean \pm s.d.

in response to *T. gondii* profilin. This notion was further supported by the lack of expression or secretion of *CCL2* or *IL12B* expression by human monocytes directly exposed to *T. gondii* profilin (Fig. 2a,b). Overall, this systems approach with human PBMCs, monocytes and an experimental THP-1 cell line infected with *T. gondii* reveals that the parasites triggered a potent chemokine response rather than inducing IL-12, a key signature of the mouse innate immune response to *T. gondii*²⁴. When combined with the lack of functional genes encoding TLR11 or TLR12 in the human genome, our results establish that innate recognition of *T. gondii* is mediated by distinct mechanisms in human and mouse myeloid cells.

Soluble mediator triggers human CCL2 response. *Toxoplasma gondii* is an obligate intracellular parasite, and the growing numbers of intracellular innate immune sensors prompted us to examine whether the infection of monocytes triggers CCL2 production in a cell-intrinsic manner. THP-1 cells were infected with mCherry-expressing parasites²⁴, and 12 h later the monocytes were

sorted and purified as either infected (mCherry⁺) cells or uninfected (mCherry⁻) cells based on the presence of the fluorescent parasite. The following quantitative rtPCR analysis of *CCL2* expression showed that both infected and uninfected monocytes produced similar amounts of CCL2 (Fig. 2c,d). In the infected mCherry⁺ cells specifically, a small but detectable induction of *IL12B* expression, but not secretion of IL-12p40, was observed (Fig. 2d), as previously reported²⁵. Taken together, these results suggest that the intracellular presence of *T. gondii* is dispensable for the induction of CCL2 by monocytes.

Host–parasite interactions lead to the presence of a third population of cells that, although not actively infected with the parasite, are exposed to parasitic molecules via contact-dependent injection of virulence factors (uninfected-injected cells)^{20,24,26,27}. To examine whether monocytic production of CCL2 requires cell contact with *T. gondii*, we monitored CCL2 expression in primary monocytes and THP-1 cells that were separated from the parasite in a transwell system. We observed that lack of direct contact between *T. gondii*

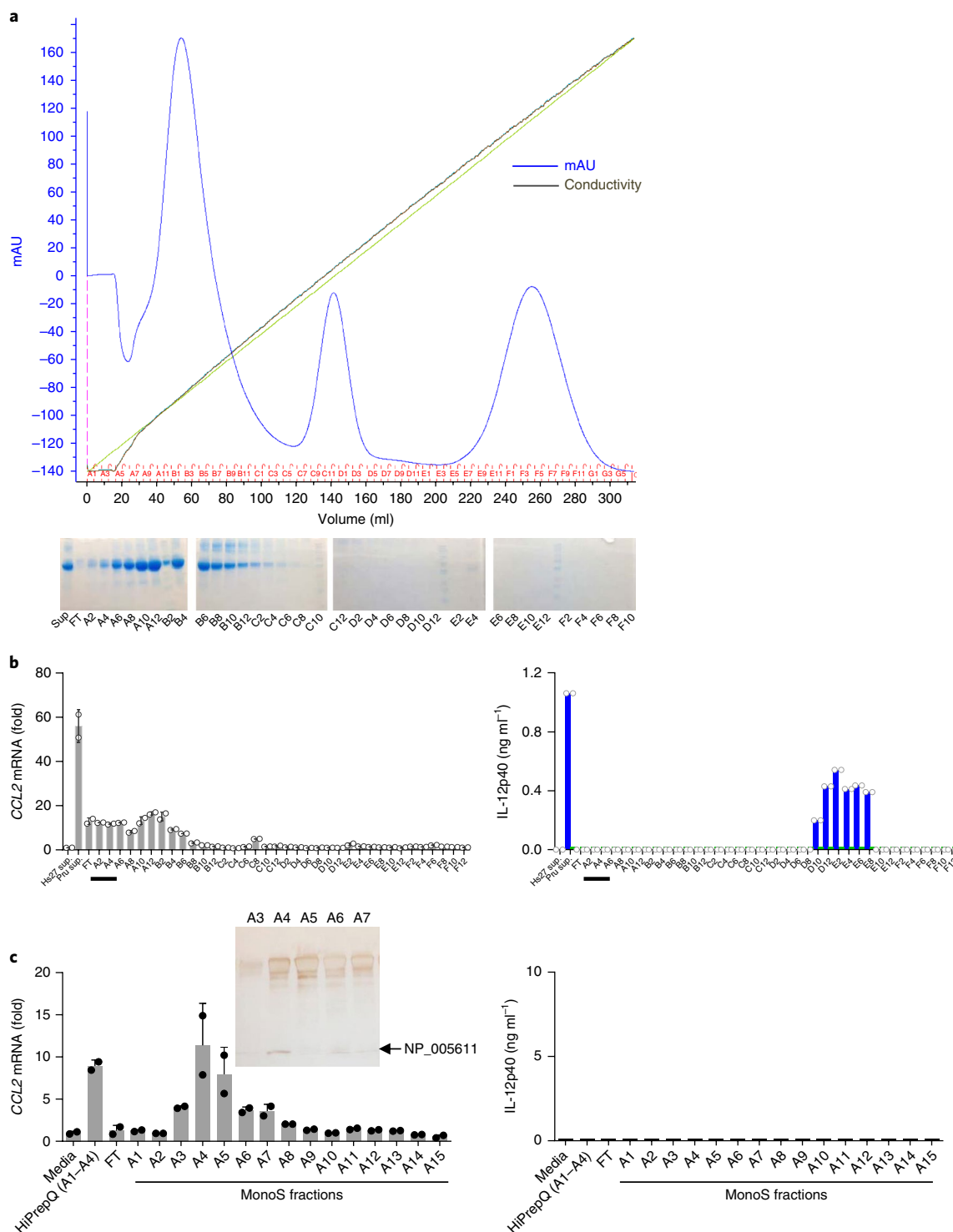


Fig. 3 | Biochemical isolation of S100A11 as a CCL2-inducing molecule. a,b, Initial separation of cell culture supernatants collected from human fibroblasts infected with the Pru strain of *T. gondii* via HiPrepQ anion-exchange chromatography (**a**) and assay of individual fractions in duplicates for their ability to induce expression of *CCL2* (**b**) in THP-1 cells (left) and to stimulate IL-12p40 secretion by mouse splenocytes prepared from wild-type (blue bars) and *Th11*^{-/-} (green bars) mice, right. mAU, milliabsorbance units. **c**, Mono S cation-exchange chromatography of fractions A1-A4 from HiPrepQ anion-exchange chromatography. Individual fractions were assayed in duplicate. Each symbol represents an individual experimental sample. Data represent five (**a,b**) or three (**c**) independent experiments; error bars represent mean ± s.d. Inset, SDS-PAGE analysis of Mono S cation-exchange chromatography fractions A3-A7; arrow indicates a band analyzed by mass spectrometry that revealed the presence of the human S100A11 protein (NP_005611).

and monocytes did not prevent induction of *CCL2* expression (Fig. 2e,f). Taken together, these results suggest that soluble mediators were responsible for *CCL2* induction in response to parasite

infection. This hypothesis was confirmed by induction of *CCL2* expression by cell culture supernatants collected from monocytes (Fig. 2e,f). Moreover, supernatants from nonimmune fibroblasts

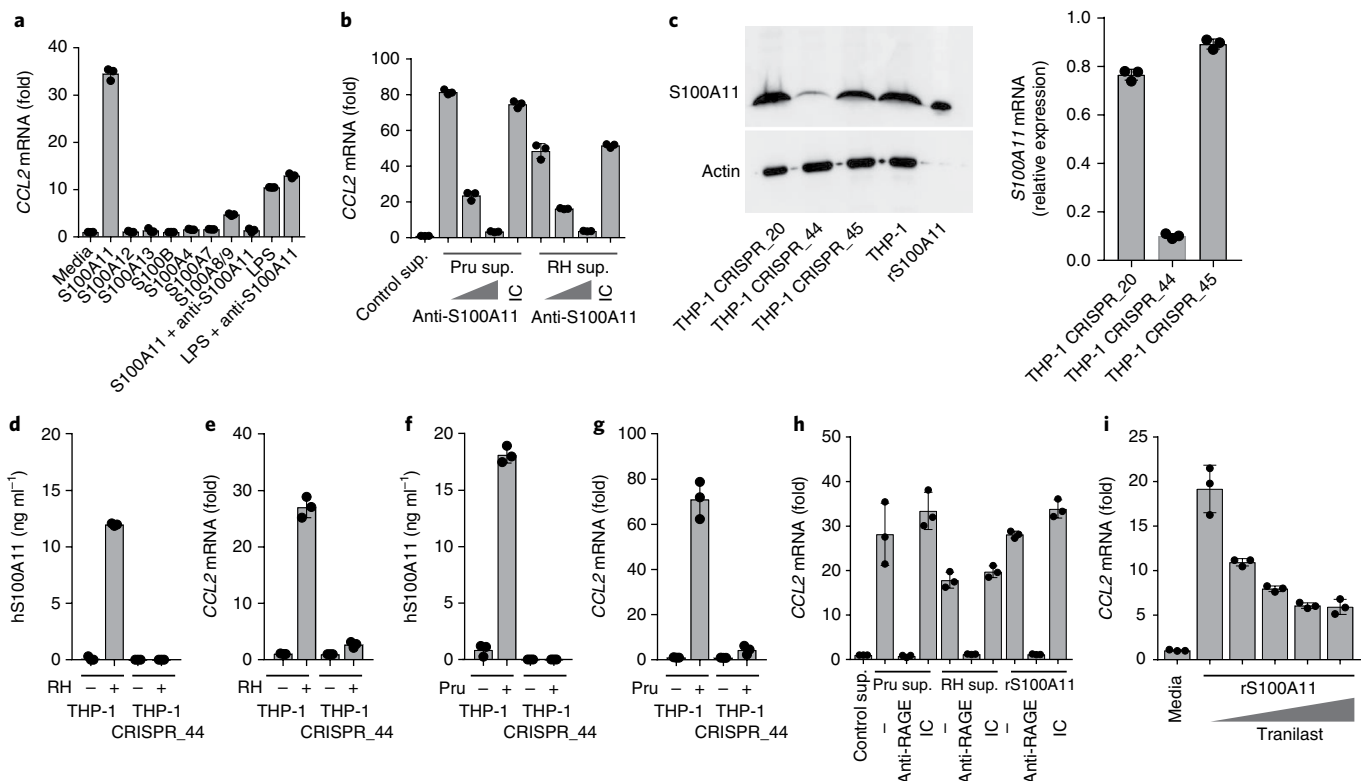


Fig. 4 | Role of RAGE in S100A11-induced CCL2. **a**, THP-1 cells were stimulated with purified recombinant S100A11, S100A12, S100A13, S100B, S100A4, S100A7 or a mixture of S100A8 and S100A9 (S100A8/9) (all at 10 ng ml^{-1}) or with lipopolysaccharide ($1 \mu\text{g ml}^{-1}$), and CCL2 expression was analyzed by rtPCR 12 h after stimulation. In several experiments, antibody to S100A11 was added to S100A11 protein (S100A11 + anti-S100A11) or to lipopolysaccharide (LPS + anti-S100A11) for 30 min before stimulation. **b**, Cell culture supernatants were collected from uninfected (control), Pru- or RH88-infected human fibroblasts and were used to stimulate monocytes directly or in the presence of increasing amounts of antibody to S100A11 or the isotype-matched control antibody (IC). CCL2 expression was analyzed by rtPCR. **c–g**, Knockdown of S100A11 in THP-1 cells (THP-1 CRISPR_44) was revealed by immunoblot and quantitative rtPCR (**c**) and resulted in loss of S100A11 release and induction of CCL2 in response to RH88 (**d,e**) and Pru (**f,g**) infections. rS100A11, recombinant S100A11. **h**, Induction of CCL2 by S100A11 or cell culture supernatants collected from *T. gondii*-infected cells was prevented by adding an antibody to RAGE but not the isotype control (IC). **i**, Induction of CCL2 by S100A11 was partially blocked by tranilast. Data represent mean \pm s.d. of assays performed in triplicate and are representative of four independent experiments.

induced CCL2 expression in THP-1 cells and primary monocytes in the transwell system; the monocytes and THP-1 cells also underwent direct activation by cell culture supernatants collected from *T. gondii*-infected cells (Fig. 2e,f). Neither control supernatants collected from uninfected cells nor recombinant *T. gondii* profilin induced CCL2 expression in human monocytes (Fig. 2e,f and data not shown). These results strongly suggest that a soluble mediator elicits CCL2 production in response to *T. gondii* infection.

Human alarmin S100A11 induces CCL2. Next, we biochemically purified a soluble mediator of CCL2 induction from cell culture supernatants of human fibroblasts infected with *T. gondii*. Anion-exchange purification showed that CCL2-inducing fractions were rapidly separated from those inducing IL-12 production from mouse splenocytes via the TLR11-mediated signaling pathway (Fig. 3a,b). These results were obtained by analysis of CCL2 expression in THP-1 cells. The *IL12B*-inducing fractions in mouse splenocytes contained *T. gondii* profilin that was released during infection and that stimulated cells via TLR11 (Fig. 3b and data not shown). These experiments establish that CCL2-inducing molecules in human cells have distinct biochemical properties from *T. gondii* profilin-initiated, TLR11-dependent induction of IL-12 by mouse cells (Fig. 3b). An additional purification step produced a relatively pure fraction, A4, that could induce potent CCL2 expression in THP-1 cells but not expression of IL-12p40 from mouse splenocytes

(Fig. 3c). Combined with the pilot experiments suggesting a low-molecular-mass protein as the CCL2-inducing molecule (data not shown), mass spectrometry of the detectable low-molecular-mass protein band was subsequently performed, leading to identification of the human S100A11 protein (Fig. 3c and Supplementary Fig. 2a). This protein belongs to a large family of small Ca^{2+} -binding proteins containing two conserved EF-hand motifs that serve pleiotropic cellular functions and can also function as a group of damage-associated mediators of inflammation^{28–31}. Sequence detection by mass spectrometry showed that S100A11 is distinct from the other S100 proteins (Supplementary Fig. 2a and data not shown).

We next directly examined whether S100A11 was sufficient for induction of CCL2. We observed that highly purified recombinant S100A11 caused potent induction of CCL2 expression in THP-1 cells (Fig. 4a). When several other S100 proteins were used in similar assays, we observed that only the S100A8–S100A9 complex could induce substantial CCL2 expression in the stimulated cells, albeit at a lower level when compared to S100A11 (Fig. 4a). In addition, we compared S100A11-induced CCL2 production with lipopolysaccharide-mediated activation of the same chemokine because recombinant S100A11 was expressed in *Escherichia coli*. We observed that large amounts of lipopolysaccharide induced relatively low amounts of CCL2 compared to those induced by S100A11 (Fig. 4a). Furthermore, an antibody to S100A11 completely prevented CCL2 induction mediated by S100A11, but not

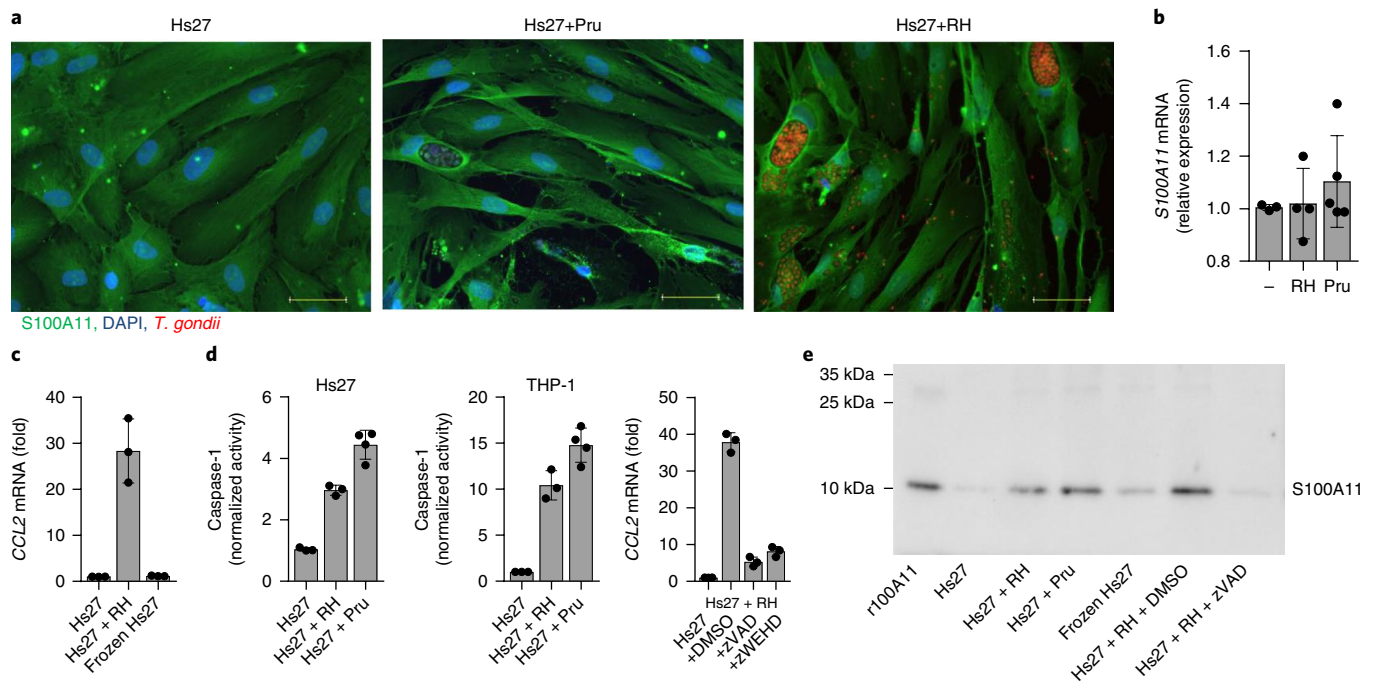


Fig. 5 | Role of caspase-1 in S100A11 release. **a,b**, Analysis of S100A11 protein levels in Pru- or RH88-infected fibroblasts by immunofluorescent detection (**a**) and by expression analysis (**b**). Scale bars, 50 μ m. Error bars represent mean \pm s.d. **c**, CCL2 expression by THP-1 cells stimulated with cell culture supernatants collected from frozen cells in comparison with RH88-infected cells. **d**, Analysis of caspase-1 activity in Hs27 and THP-1 cells infected with RH88 and Pru strains of *T. gondii*. CCL2 expression in THP-1 cells stimulated with cell culture supernatants collected from human Hs27 fibroblasts infected with RH88 alone or in the presence of zVAD (10 μ M) or zWEHD (10 μ M) for 72 h was measured by quantitative rtPCR. **e**, Detection of S100A11 in cell culture supernatants collected from Hs27 cells, Hs27 cells infected with RH88 (Hs27 + RH; MOI, 3:1) or Pru (Hs27 + Pru; MOI, 3:1), Hs27 cells killed by rapid freezing (frozen Hs27), or Hs27 cells infected with RH88 in the presence of zVAD (Hs27 + RH + zVAD). Hs27 + RH + dimethylsulfoxide (DMSO) represents an additional vehicle control supernatant for the zVAD-treated cells. Each symbol represents an individual experimental sample, $n = 3$ or $n = 4$ (**b-d**). The data shown are representative of three (**a-d**) and five (**e**) independent experiments, and error bars represent mean \pm s.d.

the induction induced by lipopolysaccharide (Fig. 4a). Taken together, these results establish that S100A11 alone can induce CCL2 expression in human monocytes. To further examine if soluble S100A11 mediated the CCL2 response, cell culture supernatants were collected from RH88- or Pru-infected fibroblasts and incubated with control antibodies or antibodies to S100A11 before stimulation of human monocytes. We observed that blocking S100A11 prevented CCL2 induction by cell culture supernatants collected from *T. gondii*-infected fibroblasts (Fig. 4b).

To examine whether S100A11 is required for CCL2 induction in response to *T. gondii* infection, we generated S100A11-deficient THP-1 cell lines using the CRISPR/Cas9 genome editing method. Stable S100A11 knockout THP-1-CRISP_44 cells did not express S100A11, as measured by immunoblot, rtPCR and enzyme-linked immunosorbent assay (ELISA), whereas wild-type THP-1 cells did express the protein (Fig. 4c,d,f and Supplementary Fig. 2b). The S100A11-deficient THP-1 cells did not produce significant amounts of CCL2 when infected with RH88 or Pru strains of *T. gondii* (Fig. 4e,g). Similarly, we observed that short interfering RNA (siRNA) sequences against S100A11 severely reduced CCL2 induction in *T. gondii*-infected cells (Supplementary Fig. 3). Collectively, these results reveal that S100A11 not only is sufficient for induction of the CCL2 response but also is required for this activity.

S100A11 induces CCL2 via RAGE. To decipher the mechanism by which S100A11 initiates the CCL2 response, we reanalyzed the RNA-seq data to identify signaling pathways that could lead to CCL2 production. The most prominent signaling pathway was a RAGE-induced cellular response to alarmins (Supplementary Figs. 4 and 5). RAGE interacts with other S100 family members^{32–34},

this prompted us to directly examine the requirement for RAGE in S100A11-mediated induction of CCL2. We found that stimulation of THP-1 cells with purified S100A11 in the presence of an antibody to RAGE, but not the isotype-matched control antibody, prevented induction of CCL2 expression (Fig. 4h). Similar results were obtained when monocytes were stimulated with cell culture supernatants collected from *T. gondii*-infected, but not control, human fibroblasts (Fig. 4h). The presence of antibodies to RAGE abrogated induction of CCL2 by cell culture supernatants produced from infected cells (Fig. 4h). In addition, CCL2 induction was diminished when monocytes were stimulated with S100A11 in the presence of tranilast, a small-molecule inhibitor of the V domain in RAGE, which is involved in interactions with S100 proteins³⁵ (Fig. 4i). These results reveal that RAGE is a key receptor that mediates S100A11-induced CCL2 production by monocytes.

Caspase-1 mediates S100A11 release. Identification of the human intracellular protein S100A11 as a mediator of the paracrine CCL2 response in *T. gondii*-infected cells raised questions regarding mechanisms regulating S100A11 release from infected cells. We first examined whether parasite invasion was required for the S100A11-mediated induction of CCL2. We observed that when *T. gondii* was rendered incapable of invasion due to profilin deficiency⁷, it did not induce S100A11-dependent induction of CCL2 expression (Supplementary Fig. 6a). Similarly, blocking parasite invasion with mycalolide B^{36,37} prevented *T. gondii*-induced induction of CCL2 in human monocytes (Supplementary Fig. 6b). These results prompted us to examine whether the cellular lysis ultimately caused by the parasite causes S100A11 release and induction of CCL2. Our experiments showed that whereas *T. gondii* infection did not change

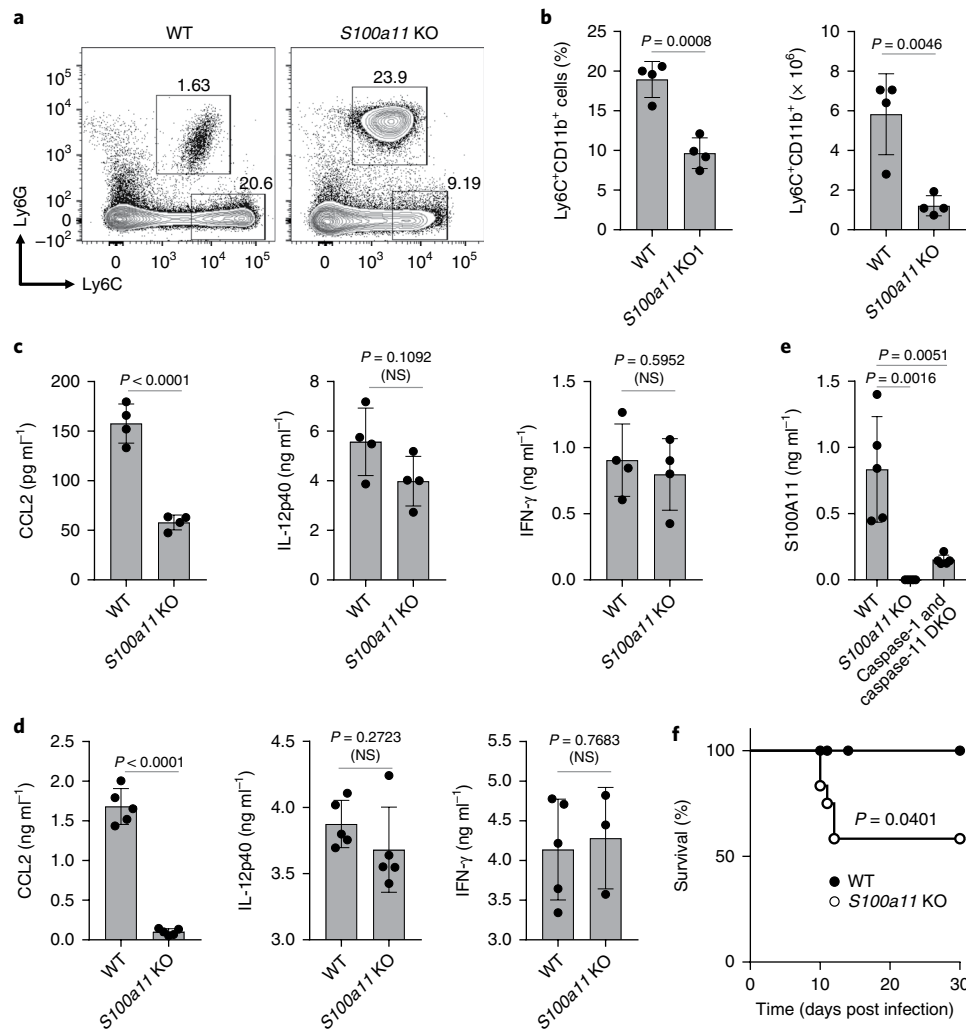


Fig. 6 | S100A11 regulates monocyte recruitment in vivo. **a**, Wild-type (WT) and *S100a11* knockout (KO) mice were infected intraperitoneally with *T. gondii*, and the presence of inflammatory monocytes and neutrophils at the site of infection was analyzed by flow cytometry on day 5 after infection. **b**, Average frequency and absolute numbers of monocytes in *T. gondii*-infected wild-type and *S100a11* knockout mice on day 5 after infection. Data are representative of four independent experiments, each involving four to six age- and sex-matched mice. **c**, CCL2, IL-12p40 and IFN- γ production were measured in the peritoneal cavity on day 5 after infection by ELISA. Data are representative of three independent experiments. **d**, CCL2, IL-12p40 and IFN- γ production were measured in sera on day 5 after infection by ELISA. Each symbol represents an individual experimental mouse. **e**, Wild-type, *S100a11* knockout, and caspase-1/caspase-11 double knockout (DKO) mice were infected intraperitoneally with *T. gondii*, and the release of S100A11 was analyzed by ELISA on day 5 after infection. Data are representative of three independent experiments. **f**, Survival of wild-type (filled circles) and *S100a11* knockout (open circles) mice infected with *T. gondii* (20 cysts per mouse). Data shown are representative of four independent experiments each involving six to eight age- and sex-matched mice. Unpaired two-tailed Student's *t*-test (**b–e**) and Mantel-Cox tests (**f**) were used for statistical analysis, NS, not significant.

the expression or abundance of S100A11 in infected or surrounding cells (Fig. 5a,b), parasite-mediated cellular damage was required for S100A11 release. Cellular death caused by rapid freezing was not sufficient for the liberation of enough S100A11 for the induction of CCL2 (Fig. 5c and Supplementary Fig. 2c). In addition, we observed not only that *T. gondii* infection led to activation of caspase-1 (Fig. 5d), but also that the pan-caspase inhibitor zVAD and the caspase-1 inhibitor zWEHD reduced S100A11 release and abolished CCL2 induction by supernatants collected from *T. gondii*-infected cells (Fig. 5d,e and Supplementary Fig. 2c). Caspase-1-deficient THP-1 cells also showed reduced production of CCL2 in response to *T. gondii* infection (data not shown). As we expected, CCL2 production by caspase-1-deficient cells was not compromised when THP-1 cells were stimulated with S100A11-containing supernatants (data not shown). Overall, these results indicate that an active cellular

response to *T. gondii* infection by an unknown intracellular receptor leads to the caspase-1-dependent release of S100A11, which is required and sufficient for the induction of CCL2.

S100A11 regulates monocyte recruitment in vivo. To examine the importance of S100A11 in the regulation of immunity to *T. gondii* in vivo, *S100A11*-deficient mice were generated (Supplementary Fig. 7) and infected intraperitoneally with *T. gondii*. We observed that a lack of *S100a11* led to compromised monocyte recruitment to the site of infection (Fig. 6a,b); this was correlated with lower concentrations of CCL2 in infected mice than in wild type mice (Fig. 6c). Concurrently, the lack of *S100a11* had no effect on the induction of the IL-12 and interferon- γ (IFN- γ) responses in vivo (Fig. 6c,d). The high concentrations of these cytokines may explain the partial role of S100A11 in host survival during intraperitoneal *T. gondii*

infection (Fig. 6f). We also observed lower concentrations of S100A11 in *T. gondii*-infected caspase-1- and caspase-11-deficient mice than in wild type mice, confirming that caspase-1 has a role in S100A11 release in vivo (Fig. 6e).

Oral infection with *T. gondii* showed that S100A11 contributes to induction of CCL2 and migration of monocytes to the site of infection, but not to the IFN- γ -mediated response to the parasite (Supplementary Fig. 8). Nevertheless, *S100a11* deficiency led to less intestinal pathology caused by the parasitic infection (Supplementary Fig. 8e,f), indicating that in addition to the protective immunity, the release of S100A11 may lead to the enhanced immunopathological response caused by *T. gondii*.

DISCUSSION

Herein, we establish a biochemical basis for the induction of the chemokine response to *T. gondii* infection by human cells. Our results show that infection with *T. gondii* leads to the release of S100A11 from infected cells. This soluble mediator is both necessary and sufficient for RAGE-dependent induction of CCL2, a major chemokine required for monocyte-mediated immunity to pathogens^{38–41}.

The previously defined mechanisms of innate immunity to *T. gondii* and closely related apicomplexan parasites are chiefly mediated by TLR11-mediated recognition of profilin, an essential molecule for the parasite invasion of host cells. TLR11-dependent innate recognition leads to rapid and selective induction of IL-12, which is required for the highly polarized T helper type 1 immunity⁴. The additional results from our and other laboratories show that TLR11 forms a heterodimer with TLR12 and detects profilin released from *T. gondii* within the endolysosomal compartment⁴. Despite clarification of the molecular events required for the TLR11-dependent activation of MyD88, a major question about TLR11-independent sensing of the parasite still remained. This gap in knowledge needed to be filled, because TLR11 and TLR12 immunity to *T. gondii* is not functional in human cells. TLR11 is encoded by a pseudogene and the gene encoding TLR12 is missing in the human genome¹³. Additional TLRs, in particular TLR2 and TLR9, as well as the NLRP1 and NLRP3 inflammasomes, are engaged by the parasite, but have a minor role in defense against *T. gondii*^{16,42}. Given the global distribution of *T. gondii* in the human population and the clinical importance of this parasite, we aimed to define innate immune sensors that could be involved in human defense against *T. gondii*.

A systems biology approach to define innate immune pathways based on the analysis of the effector molecules triggered by *T. gondii* infection, combined with biochemical screening, reveals that the human recognition system for this parasite is based on detection of the damage-associated molecule S100A11, which is released from infected cells. The human recognition system is distinct from the previously identified TLR11-mediated immune response to the parasite in mice, which depends on direct sensing of the essential *T. gondii* protein^{4,6}. A major downstream effector of S100A11-mediated activation of human monocytes is CCL2, a chemokine regulating monocyte recruitment to the site of infection⁴³. This contrasts with the soluble effector mediators released by mouse and human cells in response to *T. gondii*. Mouse dendritic cells produce large amounts of IL-12, whereas the human response to *T. gondii* is predominantly characterized by expression of CCL2. Despite biochemical differences between mice and humans in the recognition systems for *T. gondii*, both human and murine immunity to *T. gondii* rely on sensing active infection rather than the pathogen itself. This is because TLR11 detects profilin released from infected cells but not the parasite itself⁴⁴. Moreover, activation of TLR11 by *T. gondii* profilin is predominantly seen in uninfected cells⁴⁴. Similarly, human monocytes sense S100A11 released from surrounding cells infected with the parasite. This finding may represent an innate immune mechanism insensitive to an array of *T. gondii* virulence factors that can interfere with host defense pathways and determine

the outcome of infection in vivo^{20,45–47}. Consistent with this notion, the expression of S100A11 was not affected by parasite infection, suggesting that S100A11 is a pre-made alarmin that initiates rapid CCL2-mediated immune responses to the common intracellular parasite *T. gondii*.

Our in vivo results in mice suggest that the release of S100A11 from infected cells has a role in both host protection against *T. gondii* and immunopathology mediated by CCL2-dependent defense mechanisms. Additional studies are needed to determine whether S100A11-mediated immunity to *T. gondii* in humans is also primarily regulated by recruitment of monocytes to the site of infection.

Overall, our experiments reveal that human cells sense *T. gondii* by detecting infection-mediated release of S100A11. This alarmin engages RAGE and initiates signaling pathways leading to the induction of CCL2, a crucial chemokine required for host resistance to the parasite.

Online content

Any methods, additional references, Nature Research reporting summaries, source data, statements of data availability and associated accession codes are available at <https://doi.org/10.1038/s41590-018-0250-8>.

Received: 24 August 2017; Accepted: 1 October 2018;
Published online: 19 November 2018

References

- Iwasaki, A. & Medzhitov, R. Control of adaptive immunity by the innate immune system. *Nat. Immunol.* **16**, 343–353 (2015).
- Man, S. M., Karki, R. & Kanneganti, T. D. Molecular mechanisms and functions of pyroptosis, inflammatory caspases and inflammasomes in infectious diseases. *Immunol. Rev.* **277**, 61–75 (2017).
- Kawai, T. & Akira, S. The role of pattern-recognition receptors in innate immunity: update on Toll-like receptors. *Nat. Immunol.* **11**, 373–384 (2010).
- Yarovinsky, F. Innate immunity to *Toxoplasma gondii* infection. *Nat. Rev. Immunol.* **14**, 109–121 (2014).
- Pifer, R. & Yarovinsky, F. Innate responses to *Toxoplasma gondii* in mice and humans. *Trends Parasitol.* **27**, 388–393 (2011).
- Yarovinsky, F. et al. TLR11 activation of dendritic cells by a protozoan profilin-like protein. *Science* **308**, 1626–1629 (2005).
- Plattner, F. et al. *Toxoplasma* profilin is essential for host cell invasion and TLR11-dependent induction of an interleukin-12 response. *Cell Host Microbe* **3**, 77–87 (2008).
- Raetz, M. et al. Cooperation of TLR12 and TLR11 in the IRF8-dependent IL-12 response to *Toxoplasma gondii* profilin. *J. Immunol.* **191**, 4818–4827 (2013).
- Koblansky, A. A. et al. Recognition of profilin by Toll-like receptor 12 is critical for host resistance to *Toxoplasma gondii*. *Immunity* **38**, 119–130 (2013).
- Andrade, W. A. et al. Combined action of nucleic acid-sensing Toll-like receptors and TLR11/TLR12 heterodimers imparts resistance to *Toxoplasma gondii* in mice. *Cell Host Microbe* **13**, 42–53 (2013).
- Neal, L. M. & Knoll, L. J. *Toxoplasma gondii* profilin promotes recruitment of Ly6C^{hi} CCR2⁺ inflammatory monocytes that can confer resistance to bacterial infection. *PLoS Pathog.* **10**, e1004203 (2014).
- Dupont, C. D., Christian, D. A. & Hunter, C. A. Immune response and immunopathology during toxoplasmosis. *Semin. Immunopathol.* **34**, 793–813 (2012).
- Roach, J. C. et al. The evolution of vertebrate Toll-like receptors. *Proc. Natl Acad. Sci. USA* **102**, 9577–9582 (2005).
- Muller, U. B. & Howard, J. C. The impact of *Toxoplasma gondii* on the mammalian genome. *Curr. Opin. Microbiol.* **32**, 19–25 (2016).
- Debierre-Grockiego, F. et al. Activation of TLR2 and TLR4 by glycosylphosphatidylinositols derived from *Toxoplasma gondii*. *J. Immunol.* **179**, 1129–1137 (2007).
- Ewald, S. E., Chavarria-Smith, J. & Boothroyd, J. C. NLRP1 is an inflammasome sensor for *Toxoplasma gondii*. *Infect. Immun.* **82**, 460–468 (2014).
- Clay, G. M., Sutterwala, F. S. & Wilson, M. E. NLR proteins and parasitic disease. *Immunol. Res.* **59**, 142–152 (2014).
- Black, M. W. & Boothroyd, J. C. Lytic cycle of *Toxoplasma gondii*. *Microbiol. Mol. Biol. Rev.* **64**, 607–623 (2000).
- Denkers, E. Y., Schneider, A. G., Cohen, S. B. & Butcher, B. A. Phagocyte responses to protozoan infection and how *Toxoplasma gondii* meets the challenge. *PLoS Pathog.* **8**, e1002794 (2012).

20. Hakimi, M. A., Olias, P. & Sibley, L. D. *Toxoplasma* effectors targeting host signaling and transcription. *Clin. Microbiol. Rev.* **30**, 615–645 (2017).
21. Gay, G. et al. *Toxoplasma gondii* TgIST co-opts host chromatin repressors dampening STAT1-dependent gene regulation and IFN- γ -mediated host defenses. *J. Exp. Med.* **213**, 1779–1798 (2016).
22. Olias, P., Etheridge, R. D., Zhang, Y., Holtzman, M. J. & Sibley, L. D. *Toxoplasma* effector recruits the Mi-2/NuRD complex to repress STAT1 transcription and block IFN- γ -dependent gene expression. *Cell Host Microbe* **20**, 72–82 (2016).
23. Naor, A. et al. MYR1-dependent effectors are the major drivers of a host cell's early response to *Toxoplasma*, including counteracting MYR1-independent effects. *MBio* **9**, e02401-17 (2018).
24. Koshy, A. A. et al. *Toxoplasma* co-opts host cells it does not invade. *PLoS Pathog.* **8**, e1002825 (2012).
25. Tosh, K. W. et al. The IL-12 response of primary human dendritic cells and monocytes to *Toxoplasma gondii* is stimulated by phagocytosis of live parasites rather than host cell invasion. *J. Immunol.* **196**, 345–356 (2016).
26. Christian, D. A. et al. Use of transgenic parasites and host reporters to dissect events that promote interleukin-12 production during toxoplasmosis. *Infect. Immun.* **82**, 4056–4067 (2014).
27. Melo, M. B., Jensen, K. D. & Saeij, J. P. *Toxoplasma gondii* effectors are master regulators of the inflammatory response. *Trends. Parasitol.* **27**, 487–495 (2011).
28. Donato, R. S100: a multigenic family of calcium-modulated proteins of the EF-hand type with intracellular and extracellular functional roles. *Int. J. Biochem. Cell. Biol.* **33**, 637–668 (2001).
29. Donato, R. et al. Functions of S100 proteins. *Curr. Mol. Med.* **13**, 24–57 (2013).
30. Ulas, T. et al. S100-alarmin-induced innate immune programming protects newborn infants from sepsis. *Nat. Immunol.* **18**, 622–632 (2017).
31. Gross, S. R., Sin, C. G., Barraclough, R. & Rudland, P. S. Joining S100 proteins and migration: for better or for worse, in sickness and in health. *Cell. Mol. Life Sci.* **71**, 1551–1579 (2014).
32. Kierdorf, K. & Fritz, G. RAGE regulation and signaling in inflammation and beyond. *J. Leukoc. Biol.* **94**, 55–68 (2013).
33. Leclerc, E., Fritz, G., Vetter, S. W. & Heizmann, C. W. Binding of S100 proteins to RAGE: an update. *Biochim. Biophys. Acta* **1793**, 993–1007 (2009).
34. Koch, M. et al. Structural basis for ligand recognition and activation of RAGE. *Structure* **18**, 1342–1352 (2010).
35. Penumutthu, S. R., Chou, R. H. & Yu, C. Structural insights into calcium-bound S100P and the V domain of the RAGE complex. *PLoS One* **9**, e103947 (2014).
36. Hori, M. et al. Mycalolide-B, a novel and specific inhibitor of actomyosin ATPase isolated from marine sponge. *FEBS Lett.* **322**, 151–154 (1993).
37. Lavine, M. D. & Arrizabalaga, G. Exit from host cells by the pathogenic parasite *Toxoplasma gondii* does not require motility. *Eukaryot. Cell* **7**, 131–140 (2008).
38. Dunay, I. R. et al. Gr1(+) inflammatory monocytes are required for mucosal resistance to the pathogen *Toxoplasma gondii*. *Immunity* **29**, 306–317 (2008).
39. Serbina, N. V., Jia, T., Hohl, T. M. & Pamer, E. G. Monocyte-mediated defense against microbial pathogens. *Annu. Rev. Immunol.* **26**, 421–452 (2008).
40. Shi, C. & Pamer, E. G. Monocyte recruitment during infection and inflammation. *Nat. Rev. Immunol.* **11**, 762–774 (2011).
41. Kim, Y. G. et al. The Nod2 sensor promotes intestinal pathogen eradication via the chemokine CCL2-dependent recruitment of inflammatory monocytes. *Immunity* **34**, 769–780 (2011).
42. Gov, L., Schneider, C. A., Lima, T. S., Pandori, W. & Lodoen, M. B. NLRP3 and potassium efflux drive rapid IL-1 β release from primary human monocytes during *Toxoplasma gondii* infection. *J. Immunol.* **199**, 2855–2864 (2017).
43. Robben, P. M., LaRegina, M., Kuziel, W. A. & Sibley, L. D. Recruitment of Gr-1⁺ monocytes is essential for control of acute toxoplasmosis. *J. Exp. Med.* **201**, 1761–1769 (2005).
44. Pifer, R., Benson, A., Sturge, C. R. & Yarovinsky, F. UNC93B1 is essential for TLR11 activation and IL-12-dependent host resistance to *Toxoplasma gondii*. *J. Biol. Chem.* **286**, 3307–3314 (2011).
45. Saeij, J. P. et al. *Toxoplasma* co-opts host gene expression by injection of a polymorphic kinase homologue. *Nature* **445**, 324–327 (2007).
46. Reese, M. L., Zeiner, G. M., Saeij, J. P., Boothroyd, J. C. & Boyle, J. P. Polymorphic family of injected pseudokinases is paramount in *Toxoplasma* virulence. *Proc. Natl Acad. Sci. USA* **108**, 9625–9630 (2011).
47. Butcher, B. A. et al. *Toxoplasma gondii* rhoptry kinase ROP16 activates STAT3 and STAT6 resulting in cytokine inhibition and arginase-1-dependent growth control. *PLoS Pathog.* **7**, e1002236 (2011).

Acknowledgements

This work was supported by National Institute of Allergy and Infectious Diseases grants R01AI136538 and R01AI121090 and by the Burroughs Wellcome Foundation.

Author contributions

A.S. and F.Y. conceived of the study, interpreted data and wrote the manuscript; A.S. performed and analyzed all experiments, except those in Fig. 6 and Supplementary Fig. 8 (performed by A.A. and E.T.C.). E.T.C. contributed to Supplementary Fig. 7. T.J.M. and M.R.E. contributed to Supplementary Fig. 3. D.P.B. contributed to Fig. 1a,b and Supplementary Fig. 1.

Competing interests

The authors declare no competing interests.

Additional information

Supplementary information is available for this paper at <https://doi.org/10.1038/s41590-018-0250-8>.

Reprints and permissions information is available at www.nature.com/reprints.

Correspondence and requests for materials should be addressed to F.Y.

Publisher's note: Springer Nature remains neutral with regard to jurisdictional claims in published maps and institutional affiliations.

© The Author(s), under exclusive licence to Springer Nature America, Inc. 2018

Methods

Mice. To generate *S100a11*^{-/-} mice, exons 2 and 3 of the *S100A11* gene were targeted by two single-guide RNAs (sgRNAs) using CRISPR/Cas9 technology (Supplementary Fig. 7) at the Mouse Genome Editing Resource at the University of Rochester Medical Center. For genotyping, targeted alleles were detected by PCR amplification with a set of primers, S100A11 wtF (5'-GAGGCACTGCGCTCCTCTGGCACACT-3') and S100A11 wtR (5'-CTCTGCTACCAGCTTCCATGTAC-3'), resulting in PCR products of 2.7 kb for wild-type mice and 557 bp for the *S100a11* knockout allele, owing to deletion of exons 2 and 3. *S100a11* knockout mice were generated on C57BL/6 background. *S100a11* knockout mice of both sexes were born in Mendelian ratios and gained weight normally throughout development. Sex- and age-matched 6- to 12-week-old mice were used for experiments.

All mice were maintained in the pathogen-free animal facility at the University of Rochester School of Medicine and Dentistry. All animal experimentation was conducted in accordance with the guidelines of the University of Rochester University Committee on Animal Resources (UCAR) and the Institutional Animal Care and Use Committee (IACUC). All animal experimentation in this study was reviewed and approved by the University of Rochester UCAR and IACUC.

Human blood samples. PBMCs were isolated by Ficoll-plaque density-gradient centrifugation from heparinized peripheral blood of 20 healthy volunteers. All donors consented to sample donation consistent with the University of Rochester Institutional Review Board's recommendations. Both freshly purified PBMCs and those cryopreserved in liquid nitrogen were used for the study. Cryopreserved PBMCs were thawed in warm complete media (RPMI 1640, 10% FBS, penicillin-streptomycin, L-glutamine) in preparation for in vitro stimulation. All assays were performed in triplicate.

Human primary monocytes were isolated from PBMCs using CD14 MACS microbeads (Miltenyi) or purified as CD14⁺ cells from freshly prepared PBMCs.

Cell lines. THP-1 cells (TIB-202) and Hs27 fibroblasts (RL-1634) were purchased from American Type Culture Collection.

Reagents. The following siRNA targeting human S100A11 were used: sense, 5'-CUUCAUGAAUACAGAAUUAUU-3', antisense, 5'-UAGUUCUGUAUUAUGAAGUU-3' (CTM-370710); sense, 5'-UGAAGAAACUGGACACCAAUU-3', antisense, 5'-UUGGUGUCCAGUUUCUUAUU-3' (CTM-370711); sense, 5'-CAACAGUGAUGGUCAGCUAAUU-3', antisense, 5'-UAGCUGACCAUCACUGUUGUU-3' (CTM-370712); sense, 5'-GAAGUAUGCUGGAAAGGAUU-3', antisense, 5'-AUCCUUCCAGCAUACUUCUU-3' (CTM-370713). Custom-made siRNA against human *S100A11* and control siRNA were ordered from Dharmacon. The knockdown of *S100A11* in THP-1 cells was performed by CRISPR/Cas9-guided genome editing. E-CRISP, a web application (<http://www.e-crisp.org/E-CRISP/>), was used to design sgRNA sequences (S100A11_44, 5'-GCTGTCTTCCAGAAGTATGC NGG-3'; S100A11_20, 5'-GGGTCTCAGGTCCGCTTCT NGG-3'; S100A11_45, 5'-GGGTGGAGATTTTGCCTT NGG-3') cloned to lentiCRISPR v2 plasmid (Addgene, 52961) and transduced to THP-1 cells by lentivirus-mediated magnetofection (ViroMag R/L Transduction Reagent, OZ Biosciences).

Caspase-1 fluorometric assay. Caspase-1/ICE fluorometric assay kit (R&D Systems, K110-100) was used to measure caspase-1 activity in *T. gondii*-infected cells. All assays were performed in triplicate.

Toxoplasma gondii infections. For in vitro experiments, PBMCs, CD14⁺ monocytes, THP-1 or Hs27 cells were infected with RH88 or Pru *T. gondii* strains at a multiplicity of infection (MOI) of 3:1 for the indicated times. In several experiments, either a pan-caspase inhibitor or a caspase-1 inhibitor was added on day 1 after infection. We observed no effect of the inhibitors on the growth of *T. gondii* in vitro in Hs27 cells by plaque assay.

For in vivo experiments, age- and sex-matched 6- to 12-week-old wild-type and *S100a11*^{-/-} mice were intraperitoneally infected with 20 *T. gondii* brain cysts (ME49 strain) for the duration of the experiments. For the analysis of monocyte recruitment to the site of infection, peritoneal exudate cells were collected on day 5 after infection and analyzed by flow cytometry. CD11b (clone M1/70) and CD45 (clone 30-F11) antibodies were purchased from BD Bioscience; Ly6C (clone HK1.4) and Ly6G (clone 1A8) were purchased from eBioscience (Thermo Fisher).

Isolation of lamina propria cells was performed as follows. The small intestine was removed on day 7 after infection and carefully cleaned of the mesentery and Peyer patches. The intestine was then opened longitudinally, washed of fecal contents, cut into smaller sections and subjected to two sequential incubations in PBS with 5 mM EDTA and 1 mM DTT at 37 °C with agitation to remove epithelial cells. The solution was discarded between incubation steps and replaced. The remaining tissue was agitated in PBS and then filtered through a 100- μ m strainer. The tissue was then incubated for 30 min with gentle agitation in 0.4 mg ml⁻¹

collagenase D and 50 mg ml⁻¹ DNase I at 37 °C. The samples were then washed through a strainer (100 μ m).

The severity of intestinal pathology was analyzed based on the following additive scoring system⁴⁸⁻⁵⁰. For crypt and villi integrity: 0, normal; 1, irregular villi and crypts; 2, mildly inflamed; 3, severe villi and crypt loss; 4, complete villi and crypt loss with an intact epithelial cell layer; and 5, complete loss of villi and crypts and surface epithelium. For infiltration of inflammatory cells into the mucosa: 0, normal; 1, mild; 2, modest; and 3, severe. For infiltration of the submucosa: 0, normal; 1, mild; 2, modest; and 3, severe. For infiltration of the muscle: 0, normal; 1, mild; 2, modest; and 3, severe. These scores were added, resulting in a total scoring range of 0-14.

Cytokine measurements. Cytokines CCL2, IL-12p40 and IFN- γ were measured with ELISA kits (eBioscience) and by Milliplex MAP Human Cytokine/Chemokine Magnetic Bead Panel (IL-12p40, IL-12p70, IL-1 β , IL-8/CXCL8, MCP-1/CCL2, MIP-1 α /CCL3, MDC/CCL22 and MCP3/CCL7).

S100A11 isolation, purification and in vitro assays. Cell culture supernatants were collected from RH88- and Pru-infected HS27 cells cultured in complete medium (RPMI 1640, 10% FBS, penicillin-streptomycin and L-glutamine). The cell culture supernatants were first filtered through a 0.22 μ m filter and then separated by a HiPrepQ chromatography column by applying a linear gradient of 0-1 M NaCl in 20 mM Tris, pH 8.0. The collected fractions were analyzed on 12% SDS-polyacrylamide gel electrophoresis (SDS-PAGE) gels (Bio-Rad) and tested for their ability to trigger CCL2 expression in THP-1 cells. The active fractions A1-A4 were pooled and subjected to cation-exchange chromatography on a Mono S column. The active fast protein liquid chromatography fractions were analyzed by SDS-PAGE and subjected to mass spectrometry-mass spectrometry analysis. The identified S100A11 peptides are shown in Supplementary Fig. 2a.

For protein expression, the synthetic *S100A11* gene (NM_005620) was prepared at Integrated DNA Technologies and inserted into the pET-17b vector (Novagen) using its NdeI and XhoI restriction sites, and then expressed in *E. coli* strain BL21(DE3) pLysS cells. The resulting recombinant protein was purified to homogeneity (as judged by SDS-PAGE) by a combination of anion-exchange and Sephacryl S-100 chromatography. Lipopolysaccharide levels in the recombinant protein preparations were analyzed using the LAL Chromogenic Endotoxin Quantification kit (Thermo) per the manufacturer's instructions.

The CCL2-inducing activity of cell culture supernatants and recombinant S100A11 protein was assayed by THP-1 cells, PBMCs or CD14⁺ monocytes with serial dilutions of the test sample, followed by RNA extraction and measurement of CCL2 and *IL12B* expression by rtPCR.

For immunofluorescence, control and *T. gondii*-infected cells were fixed in 4% paraformaldehyde in PBS for 4 h. Cells were permeabilized with 0.2% Triton-X in PBS, and blocked with 0.1% Triton-X with 5% normal goat serum in PBS. Permeabilized cells were incubated with rabbit polyclonal antibody to S100A11 followed by secondary Alexa Fluor 488 conjugated antibody (GE Healthcare) for 1 h at room temperature, and counterstained with 4,6-diamidino-2-phenylindole (DAPI). Slides were imaged with an inverted microscope (Leica DMi8) using a Leica \times 40 objective.

Quantitative real-time PCR. Total RNA was isolated from experimental cells using a Purelink RNA mini kit (Life Technologies) and subjected to first-strand cDNA synthesis using an iScript Reverse Transcription Supermix for quantitative rtPCR (Bio-Rad). Real-time PCR was performed using Ssofast Eva Green Supermix (Bio-Rad). The relative expression of each sample was determined after normalization to the housekeeping gene *GAPDH* using the relative ddCt rtPCR quantification method. The following primers were used for gene expression analysis: *GAPDH*, 5'-GAGCCCGCAGCCTCCCGCTT-3' and 5'-CCCGCGCCATCACGCCACAG-3'; *CCL2*, 5'-CCCCAGTCACCTGCTGTAT-3' and 5'-TGGAACTCTGAACCCACTTC-3'; and *IL12B*, 5'-AGAGGCTCTTCTGACCCCCAAG-3' and 5'-CTCTTGTCTTGCCCTGGACCTG-3'.

RNA-seq data and signaling pathway analyses. Five randomly chosen human PBMC samples (out of $n = 20$) were prepared for RNA-seq experiments. For each sample, PBMCs were divided into three aliquots (0.5×10^6 cells per sample) and were (1) left untreated, (2) infected with *T. gondii* Pru strain at MOI of 3, or (3) infected with *T. gondii* RH strain at MOI of 3. After 12 h after infection, 15 samples were subjected to RNA sequencing. Total RNA was extracted and used for library preparation according to the manufacturer's protocols. Samples were sequenced on the Illumina HiSeq 1000 with 20×10^6 80-bp single-read per sample. Raw reads were analyzed within the Galaxy platform, trimmed for adaptor sequence, masked for low-complexity or low-quality sequences, then mapped to the hg38 assembly of the whole human genome using TopHat v2.1.0 (default parameters) and analyzed by Cuffdiff v2.2.1 (default parameters) for differential gene expression between *T. gondii*-infected and uninfected samples. The results of the RNA-seq data analysis pipeline were uploaded to Ingenuity Pathway Analysis software to identify signaling pathways shown in Supplementary Figs. 4 and 5. The pheatmap R package was used to build heatmaps where the genes were filtered to

satisfy the following conditions: (1) for at least one sample, expression values in units of fragments per kilobase of transcript per million mapped reads were >200 in one or more conditions (infected or uninfected), and (2) fold change ≥ 4 . Only genes with logarithmic fold differences >2 were used for heatmaps. Accession code: RNA-seq data, GSE119835.

Statistical analysis. All data were analyzed with Prism (version 6; Graphpad). These data were considered statistically significant for $P < 0.05$ by two-tailed t -test.

Reporting Summary. Further information on research design is available in the Nature Research Reporting Summary linked to this article.

Data availability

The materials, data, and any associated protocols that support the findings of this study are available from the authors upon reasonable request. All RNA-seq data

generated in this study have been deposited in the Gene Expression Omnibus (GEO) under accession code GSE119835.

References

48. Burger, E. et al. Loss of Paneth cell autophagy causes acute susceptibility to *Toxoplasma gondii*-mediated inflammation. *Cell Host Microbe* **23**, 177–190.e4 (2018).
49. Lopez-Yglesias, A. H., Burger, E., Araujo, A., Martin, A. T. & Yarovinsky, F. T-bet-independent Th1 response induces intestinal immunopathology during *Toxoplasma gondii* infection. *Mucosal Immunol.* **11**, 921–931 (2018).
50. Raetz, M. et al. Parasite-induced TH1 cells and intestinal dysbiosis cooperate in IFN- γ -dependent elimination of Paneth cells. *Nat. Immunol.* **14**, 136–142 (2013).

Reporting Summary

Nature Research wishes to improve the reproducibility of the work that we publish. This form provides structure for consistency and transparency in reporting. For further information on Nature Research policies, see [Authors & Referees](#) and the [Editorial Policy Checklist](#).

Statistical parameters

When statistical analyses are reported, confirm that the following items are present in the relevant location (e.g. figure legend, table legend, main text, or Methods section).

n/a Confirmed

- The exact sample size (n) for each experimental group/condition, given as a discrete number and unit of measurement
- An indication of whether measurements were taken from distinct samples or whether the same sample was measured repeatedly
- The statistical test(s) used AND whether they are one- or two-sided
Only common tests should be described solely by name; describe more complex techniques in the Methods section.
- A description of all covariates tested
- A description of any assumptions or corrections, such as tests of normality and adjustment for multiple comparisons
- A full description of the statistics including central tendency (e.g. means) or other basic estimates (e.g. regression coefficient) AND variation (e.g. standard deviation) or associated estimates of uncertainty (e.g. confidence intervals)
- For null hypothesis testing, the test statistic (e.g. F , t , r) with confidence intervals, effect sizes, degrees of freedom and P value noted
Give P values as exact values whenever suitable.
- For Bayesian analysis, information on the choice of priors and Markov chain Monte Carlo settings
- For hierarchical and complex designs, identification of the appropriate level for tests and full reporting of outcomes
- Estimates of effect sizes (e.g. Cohen's d , Pearson's r), indicating how they were calculated
- Clearly defined error bars
State explicitly what error bars represent (e.g. SD, SE, CI)

Our web collection on [statistics for biologists](#) may be useful.

Software and code

Policy information about [availability of computer code](#)

Data collection

FPLC: UNICORN 7 (GE Healthcare Life Sciences). Flow cytometry: BD FACS Diva 8.0.1

Data analysis

RNA Seq: Reads were trimmed by a Trimmomatic program after quality control checks on raw sequence data by FastQC. The alignment of reads to the human genome was performed by the TopHat program followed by Cuffdiff execution to find significant changes in transcript expression between treated and untreated samples. The results of the RNAseq data analysis pipeline were uploaded to IPA software to identify signaling pathways.
Graphs and statistical analysis: Graph Prism
Flow cytometry: BD FACS Diva 8.0.1, FlowJo v.10

For manuscripts utilizing custom algorithms or software that are central to the research but not yet described in published literature, software must be made available to editors/reviewers upon request. We strongly encourage code deposition in a community repository (e.g. GitHub). See the Nature Research [guidelines for submitting code & software](#) for further information.

Data

Policy information about [availability of data](#)

All manuscripts must include a [data availability statement](#). This statement should provide the following information, where applicable:

- Accession codes, unique identifiers, or web links for publicly available datasets
- A list of figures that have associated raw data
- A description of any restrictions on data availability

The materials, data, and any associated protocols that support the findings of this study are available from the corresponding authors upon request.

Field-specific reporting

Please select the best fit for your research. If you are not sure, read the appropriate sections before making your selection.

Life sciences Behavioural & social sciences Ecological, evolutionary & environmental sciences

For a reference copy of the document with all sections, see [nature.com/authors/policies/ReportingSummary-flat.pdf](https://www.nature.com/authors/policies/ReportingSummary-flat.pdf)

Life sciences study design

All studies must disclose on these points even when the disclosure is negative.

Sample size	No sample size calculation was performed. The exact n values used to calculate the statistics are provided and a reasonable sample size was chosen to ensure adequate reproducibility of results.
Data exclusions	No data were excluded from the analysis. For RNAseq data, only genes with the expression values in FPKM>200 were shown. We did not show genes with the lower FPLM values due to their low levels of expression, but all data will be available and are not excluded.
Replication	Experiments were replicated several times (3-5) with reproducible results, as indicated in each figure legend.
Randomization	Figure 1: Random anonymous donors (n=5) Figure 2: Not applicable, we tested the defined chemical compounds Figure 3: Not applicable, we tested the defined biochemical fractions Figure 4: Not applicable, we tested the defined chemical compounds Figure 5: Not applicable. Figure 6: Age- and sex-matched mice were separated as WT and S100a11 KO. Mice were co-housed to minimize the microbiota effects.
Blinding	Figures 1-5: not blinded Figure 6: The investigator was blinded (the genotypes were not revealed prior T. gondii infection).

Reporting for specific materials, systems and methods

Materials & experimental systems

n/a	Involvement in the study
<input checked="" type="checkbox"/>	<input type="checkbox"/> Unique biological materials
<input type="checkbox"/>	<input checked="" type="checkbox"/> Antibodies
<input type="checkbox"/>	<input checked="" type="checkbox"/> Eukaryotic cell lines
<input type="checkbox"/>	<input checked="" type="checkbox"/> Palaeontology
<input type="checkbox"/>	<input checked="" type="checkbox"/> Animals and other organisms
<input checked="" type="checkbox"/>	<input type="checkbox"/> Human research participants

Methods

n/a	Involvement in the study
<input checked="" type="checkbox"/>	<input type="checkbox"/> ChIP-seq
<input type="checkbox"/>	<input checked="" type="checkbox"/> Flow cytometry
<input checked="" type="checkbox"/>	<input type="checkbox"/> MRI-based neuroimaging

Antibodies

Antibodies used

S100A11 Abs: generated against highly purified recombinant S100A11 protein.
hCCL2 (Cat #14-7099-68, lot E05354_1635) and IL-12p40 (cat #14-7125-68, lot E05380-1635) ELISA kit antibodies were purchased from eBiosciences.
anti-RAGE antibody (Cat #AF1179, lot GWZ0416081) and rh-RAGE/Fc reagent (Cat #1145-RG, lot #FAU0714061) were purchased from R&D Systems.

CD11b antibodies (clone M1/70, cat # 557872, lot 5009911) were purchased from BD Bioscience.
 CD45 antibodies (clone 30-F11, cat # 565967, lot 8037968) were purchased from BD Bioscience;
 Ly6C antibodies (clone HK1.4, cat# 45-5932-82, lot E10161-1634) were purchased from eBioscience
 Ly6G antibodies (clone 1A8, cat # 17-9668-82, lot 4286053) were purchased from eBioscience (ThermoFisher).

Validation

S100A11 Abs validated for specificity against the following control proteins: A100A1, A12, A13, A4, A7, A8, A9 proteins (no reactivity).
 CCL2 and IL-12p40 Abs (eBiosciences) were validated by the vendor and extensively characterized in the past by our lab.
 RAGE Abs: these Abs blocked RAGE-induced activation caused by a previously described unrelated RAGE-ligand (HMGB1)
 All the flow cytometry antibodies used are from commercial sources and have been validated by the vendors. Validation data are available on the manufacturer's website.

Eukaryotic cell lines

Policy information about [cell lines](#)

Cell line source(s)

THP-1 cells (TIB-202) and Hs27 fibroblasts (RL-1634) were purchased from ATCC.

Authentication

THP-1 and Hs27 cells were authenticated by morphology

Mycoplasma contamination

THP-1 cells (TIB-202) and Hs27 fibroblasts (RL-1634) were routinely tested for mycoplasma (every 4 weeks). All results were negative

Commonly misidentified lines
(See [ICLAC](#) register)

No misidentified cells were involved in the experiments.

Palaeontology

Specimen provenance

Provide provenance information for specimens and describe permits that were obtained for the work (including the name of the issuing authority, the date of issue, and any identifying information).

Specimen deposition

Indicate where the specimens have been deposited to permit free access by other researchers.

Dating methods

If new dates are provided, describe how they were obtained (e.g. collection, storage, sample pretreatment and measurement), where they were obtained (i.e. lab name), the calibration program and the protocol for quality assurance OR state that no new dates are provided.

Tick this box to confirm that the raw and calibrated dates are available in the paper or in Supplementary Information.

Animals and other organisms

Policy information about [studies involving animals](#); [ARRIVE guidelines](#) recommended for reporting animal research

Laboratory animals

All mice used for experiments were on a C57BL/6J genetic background and 6-12 weeks-old.

To generate S100a11^{-/-} mice, exons 2 and 3 of the S100a11 gene were targeted by two sgRNAs using CRISPR-Cas9 technology (Supplementary Fig. 7) at the Mouse Genome Editing (MGE) Resource at the University of Rochester Medical Center. Genotyping of S100a11^{-/-} mice was performed using primers S100a11 wtF (5'-gaggcactgctcctctggcacact-3') and S100a11 wtR (5'-ctcctgctaccagcttccatgtcac-3') that result in PCR products of 2.7 kb for WT mice and 557 bp for the S100a11 KO allele, as a result of deletion of exons 2 and 3.

C57BL/6 mice were initially purchased from the Jackson Labs and were bred at the University of Rochester.

Wild animals

The study did not involve wild animals

Field-collected samples

The study did not involve samples collected from the field.

Plots

Confirm that:

- The axis labels state the marker and fluorochrome used (e.g. CD4-FITC).
- The axis scales are clearly visible. Include numbers along axes only for bottom left plot of group (a 'group' is an analysis of identical markers).
- All plots are contour plots with outliers or pseudocolor plots.
- A numerical value for number of cells or percentage (with statistics) is provided.

Methodology

Sample preparation

Isolation of lamina propria cells was performed as follows. The small intestine was removed on day 7 post infection and carefully cleaned of the mesentery and Peyer patches. The intestine was then opened longitudinally, washed of fecal contents, cut into smaller sections and subjected to 2 sequential incubations in PBS with 5 mM EDTA and 1mM DTT at 37°C with agitation to remove epithelial cells. The solution was discarded between incubation steps and replaced. The remaining tissue was agitated in PBS and then filtered through a 100-µm strainer. The tissue was then incubated for 30 min with gentle agitation in 0.4 mg/ml of Collagenase D and 50 mg/ml of DNase I at 37 °C. The samples were then washed through a strainer (100 µm). Peritoneal exudate cells were collected on day 5 post infection

Instrument

BD LSRII

Software

BD FACS Diva 8.0.1 software was used for data collection and FlowJo v.10 was used for data analysis.

Cell population abundance

Post-sort cells were analyzed on BD LSRII and the purity of CD14+ cells was at least 98.5%

Gating strategy

Among live, single, CD45+ cells,
Neutrophils were gated as: CD11b+Ly6G+Ly6C-
Monocytes were gated as CD11b+Ly6C+Ly6G-

- Tick this box to confirm that a figure exemplifying the gating strategy is provided in the Supplementary Information.